

## EFFECT OF WATER VAPOR ON THE REDUCTION KINETICS OF HEMATITE POWDER BY HYDROGEN-WATER VAPOR IN DIFFERENT STAGES

X.-D. Mao, X.-J. Hu\*, Y.-W. Fan, K.-C. Chou

University of Science and Technology Beijing, State Key Laboratory of Advanced Metallurgy, Beijing, P.R. China

(Received 23 May 2022; Accepted 17 January 2023)

### Abstract

The powder of the hematite sample was isothermally reduced with a hydrogen-water vapor gas mixture at 1023K-1273K. The results indicate that the overall reduction process of hematite can be divided into three stages ( $Fe_2O_3$ - $Fe_3O_4$ - $FeO$ - $Fe$ ) each of which should be investigated. At 1023K, the average reaction rate decreased by 53.6% in stage 1 when the water vapor content of the reaction gas increased from 0% to 50%, and it decreased by about 77.2% in stage 2. However, in stage 3, when the water vapor content increased only from 0% to 20%, it decreased by about 78.1%. The results also show that the influence of water vapor on the reduction reaction increases with increasing reaction temperature in all stages of the reduction reaction. The microstructure of the reduction products showed that they still had some holes; that did not seriously block the channel for hydrogen diffusion. Various models were considered to further clarify the influence of water vapor in the reduction stage. The range of apparent activation energy of the different stages obtained by the model fitting was about 20-70 kJ/mol, which also confirmed the absence of the solid-state diffusion phenomenon.

**Keywords:** Reduction; Water; Hydrogen; Kinetics mechanism

### 1. Introduction

The steel industry is an energy-intensive industry, its energy consumption accounts for 5% of the world's total energy consumption [1-2], and the  $CO_2$  emissions in the production process of steel are huge. According to relevant information and reports [3], on average, about 1.8t of carbon dioxide will be emitted for every ton of steel produced. Global steel production was 1.878 billion tons in 2020, the annual  $CO_2$  emissions of the world's steel industry are about 3.38 billion tons, so it is particularly important to reduce  $CO_2$  emissions in the steel industry. If shaft furnace used  $H_2$  direct ironmaking instead of blast furnace ironmaking in steel industry,  $CO_2$  emissions could be greatly reduced [4-6].

In the process of hydrogen reduction of iron ore (e.g. shaft furnace), the water content in hydrogen continues to rise, and the gas mixture with high water vapor content can only reduce iron ore with low reduction degree [7], which means that the influence of water vapor is not negligible. This is a consecutive reduction process, and many reduction kinetics problems need to be studied further. Guo et al. [8] claimed a stepwise reduction sequence of  $Fe_2O_3 \rightarrow FeO \rightarrow Fe$  was observed during the reduction process with biomass-derived syngas at temperatures

1123K-1323K. Kim et al. [9] studied the retardation kinetics of cylindrical compacts of magnetite reduction, and reported that the presence or absence of retardation is hugely related to the conditions of the reaction. Adam et al. [10] consider OH groups trap  $Fe^{2+}$  ions which make nucleation easier and more uniform and growth is slowed because active sites are blocked by water. Moreover, the reaction was considerably retarded by the water produced with hydrogen at 300°C-400°C. Moukassi et al. [11] determined that water vapor has a large retarding effect in the reduction of wustite by hydrogen at 600°C-950°C. The research of Garg et al. [12] showed that the products formed by reduction with  $H_2$ - $H_2O$  gas mixture containing higher mole fraction of  $H_2O$  were sintered more seriously at high temperature. Steffen et al. [13] investigated the growth rate of iron nuclei on magnetite in a hydrogen-water vapor-argon gas mixture atmosphere, and the results showed that the growth rate of iron nuclei decreased rapidly with the slight increase of water vapor content in the gas mixture. In the previous research on the reduction of iron ore with hydrogen, there are relatively few studies on hydrogen containing water vapor as gas reactant, and these studies mainly focus on the effect of water vapor on the growth of iron nuclei or the effect of water vapor on the overall reduction

\*Corresponding author: huxiaojun@ustb.edu.cn



situation. In order to better understand the consecutive reduction process of iron ore by hydrogen, this study divides the whole reduction process into three stages and then investigates the effect of water vapor on each stage separately. Therefore, in this study, hematite powder was used to react with hydrogen-water vapor gas mixture in different proportions to achieve the research purpose. Once the effect of water vapor on the reduction of iron ore by hydrogen is known, the operating parameters of hydrogen reduction ironmaking can be improved to reduce the production cost and increase the production efficiency.

## 2. Materials and methods

The hematite sample used in this investigation was provided by calcining reagent grade  $\text{Fe}_2\text{O}_3$ , which was detected by the laser particle size analyzer (CLF-2, Malvern) to determine the distribution particle size and the result shown 95% particle size was less than  $10\mu\text{m}$  and it stored in vacuum drying oven and dehydrated for 48 hours before the experiment, and the X-ray diffraction pattern of the hematite sample is shown in Figure 1. The experiment was conducted using a thermo-gravimetric analyzer (TGA, HCT-4, Henven); the mass loss was recorded at 1 Hz, and TGA had a precision of  $\pm 1\mu\text{g}$ . The hematite sample was put into the crucible and spread into a thin layer. The inner diameter of the alumina crucibles used in the experiment were 16mm; the crucibles were cleaned by an ultrasonic cleaner and then dried in vacuum drying oven before use. The mass flowmeter (Alicat) which has an accuracy of  $\pm 0.5\%$  was used to control the gas flow rate. The part about water of hydrogen-water vapor gas mixture was controlled by the appliance provided by Bronkhorst. A schematic diagram of the experimental apparatus is given in Figure 2.

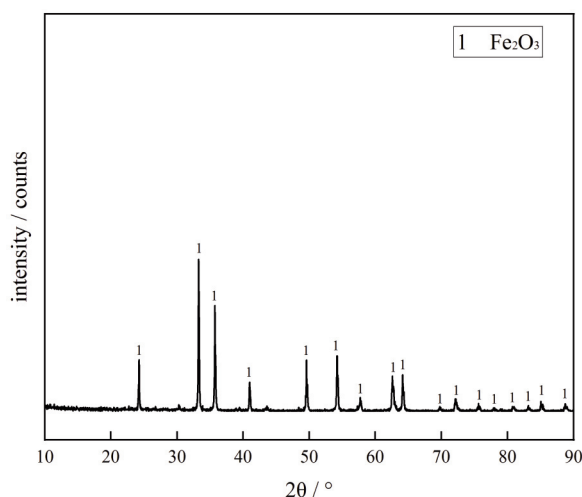


Figure 1. X-ray diffraction pattern of the hematite sample

The hematite sample was isothermally reduced with hydrogen and hydrogen-water vapor gas mixture at 1023K-1273K. In all the reduction experiments, 0.1g of hematite sample was placed in the TGA heated to the desired temperature under argon atmosphere (purity of 99.999%), the gas mass flow rate was 40sccm. When the temperature was reached, the argon was switched to hydrogen or hydrogen-water vapor gas mixture; the experimental condition of gas reactant composition is given in Table 1, and the gas mass flow rate continued to be 40sccm. Moisture in argon was removed by passing through a column of silica. After the reduction reaction, the hydrogen or hydrogen-water vapor gas mixture was switched to argon until the sample was cooled to room temperature. The weight of the hematite sample was continuously measured by the TGA. The X-ray diffraction (XRD, SmartLab, Rigaku) and the scanning electron microscope (SEM, MLA250, FEI) were used to characterize the different phases and the structure of reduction product.

## 3. Results and discussion

### 3.1. Experiment results

In this experiment, the mass change of the hematite sample during the reduction process is considered to be caused by the “deprivation” of oxygen in the sample by hydrogen. Therefore, the reduction degree (conversion degree)  $X$  of hematite is defined as the ratio of the mass of oxygen in the hematite that has been reacted at time  $t$  to the mass of oxygen in the hematite in the original sample.

$$X = \frac{m_i - m_t}{m_i - m_\infty} \quad (1)$$

where  $m_i$ ,  $m_t$ ,  $m_\infty$  are the mass of sample in the initial, the mass of sample at the time  $t$ , the mass of the complete reaction of hematite, respectively. The average reaction rate can be obtained by the

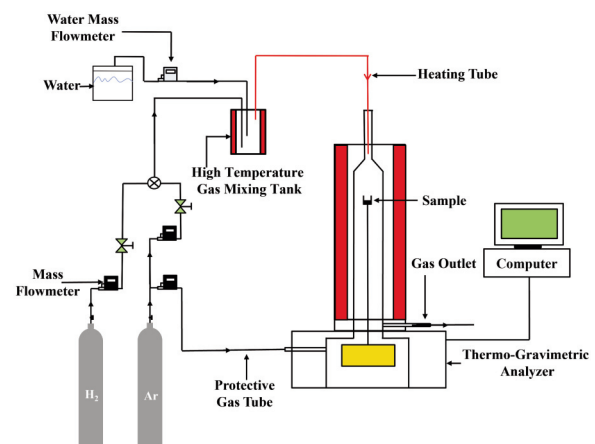


Figure 2. The schematic diagram of the experimental setup

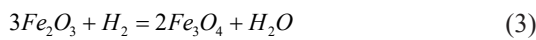
**Table 1.** Experimental conditions of isothermally reduction reaction

| No. | Temperature, K | Gas reactant, atm |                  |
|-----|----------------|-------------------|------------------|
|     |                | H <sub>2</sub>    | H <sub>2</sub> O |
| 1   | 1023           | 0.5               | 0.5              |
| 2   | 1023           | 0.8               | 0.2              |
| 3   | 1023           | 0.9               | 0.1              |
| 4   | 1023           | 1                 | 0                |
| 5   | 1073           | 0.5               | 0.5              |
| 6   | 1073           | 0.8               | 0.2              |
| 7   | 1073           | 0.9               | 0.1              |
| 8   | 1073           | 1                 | 0                |
| 9   | 1173           | 0.5               | 0.5              |
| 10  | 1173           | 0.8               | 0.2              |
| 11  | 1173           | 0.9               | 0.1              |
| 12  | 1173           | 1                 | 0                |
| 13  | 1273           | 0.5               | 0.5              |
| 14  | 1273           | 0.8               | 0.2              |
| 15  | 1273           | 0.9               | 0.1              |
| 16  | 1273           | 1                 | 0                |

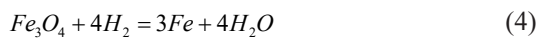
following formula,

$$v = \frac{\Delta X}{\Delta t} \quad (2)$$

In general, hematite is not directly reduced to iron by gas reduction [14-17]. In the first instance, it forms lower-valence oxides, and then turns into metallic iron through lower-valence oxides according to the thermodynamic phase diagram (Figure 3) and the following equations [14, 18], and the Gibbs free energy change of each reaction is shown in Figure 4.



$$T < 821\text{K}$$



$$T > 821\text{K}$$



Since a small number of sites (1-x) in the wustite lattice are not occupied by iron ions, the wustite in the above equation is written as Fe<sub>x</sub>O [19]. Wustite is unstable at low temperatures under thermodynamic equilibrium, but when the temperature is higher than 821K, there is a stable area of wustite [20]. Since the

temperature in this experiment is higher than the critical temperature of 821K, the reduction route of hematite is first to be reduced to magnetite by hydrogen or hydrogen-water vapor gas mixture and then reduced to wustite and finally reduced to iron. Meanwhile, the sample particles selected in the experiment were too small to be understood as layered reduction, but should be considered as a staged reduction.

The reduction of hematite to iron required three stages during experimental temperature. In general, for hematite reduction reaction, the reduction from wustite to metallic iron is the control stage among three reduction stages, hence it can be considered that the rate of reduction from hematite to magnetite and magnetite to wustite are relatively fast [21-22]. Figure 5 shows the results of reduction reaction of hematite powder at 1023K-1273K. For pure hydrogen, achieving about 100% the reduction degree would take at least 2000s at 1023K. However, it would have taken only 800s to reach about 100% the degree of

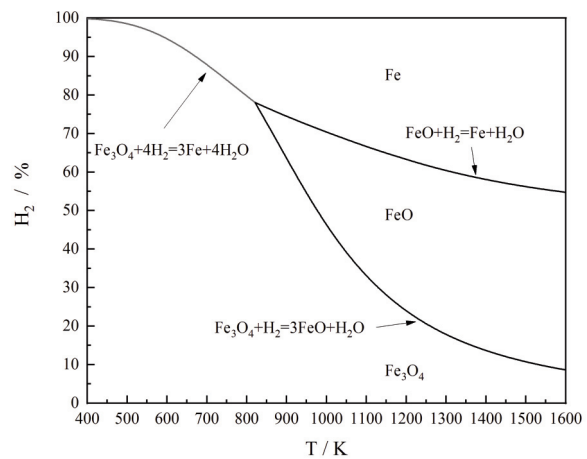


**Figure 3.** The thermodynamic phase diagram of Fe-O-H system equilibrium at 1 atm (calculated with FactSage7.0)

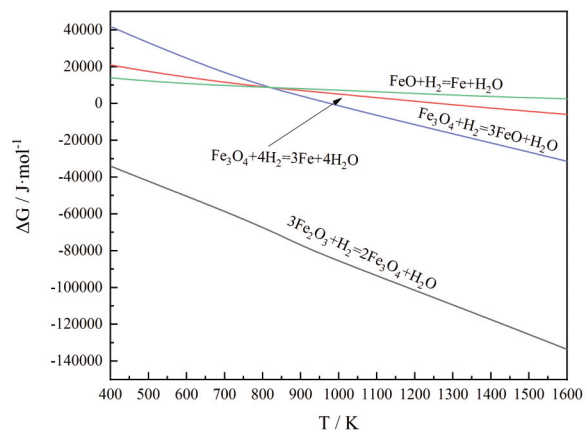


**Figure 4.** The Gibbs free energy change of each reaction (calculated with FactSage7.0)



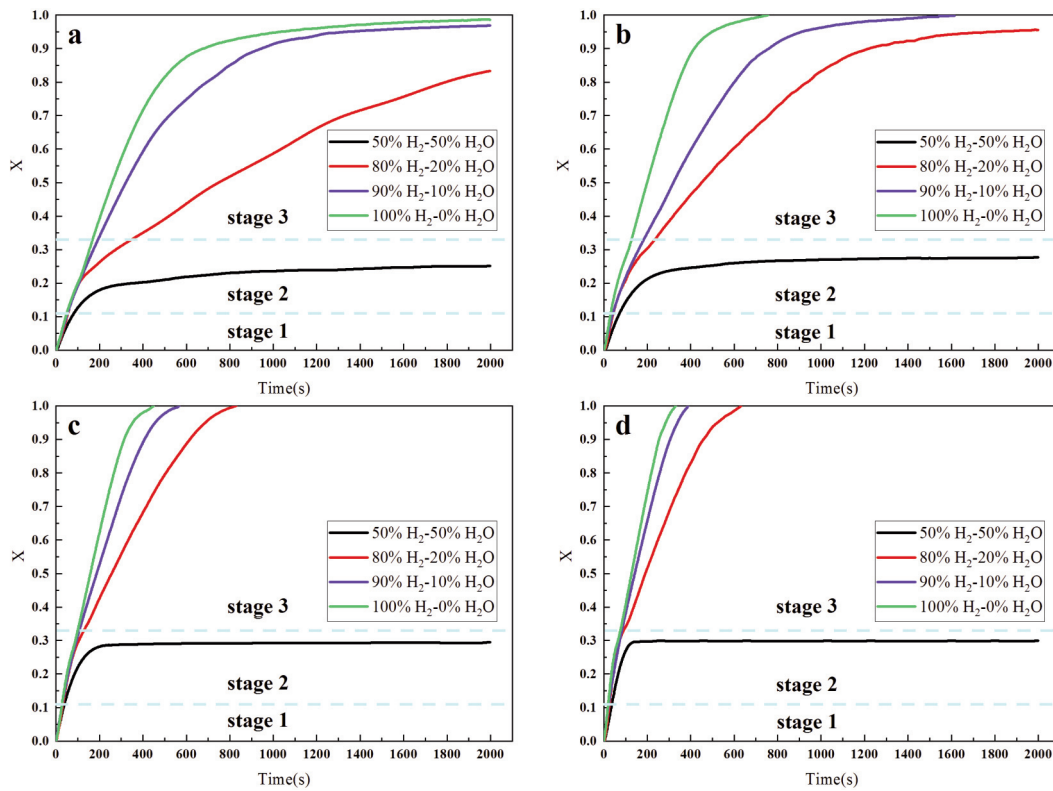


Figure 5. Reduction degree curves for hematite at (a) 1023K (b) 1073K (c) 1173K (d) 1273K

reduction by increasing the temperature to 1073K, which would have cut the time at least by half. As the experimental temperature continued to increase, the time required for the reaction was further reduced. On the other hand, the reaction time increased as the content of water vapor in the gas reactant increased. When the water vapor content was further increased to 50%, the hematite powder could only be reduced to wustite, but its reduction curve of the stage 1 was also roughly consistent with the overall reduction trend. This phenomenon indicates that the stage 1 of hematite sample powder reduction is less affected by water vapor, which is also consistent with the study of Lorente [23].

### 3.2. Effect of water on the reduction degree

Water vapor, as the product of hydrogen and iron oxide reduction reaction, is mixed with hydrogen gas in a certain proportion as the gas reactant that is introduced into the reactor for reduction reaction with hematite sample, and there is no doubt that water vapor will affect the reaction process. As shown in Figure 6, the gas reactant containing only pure hydrogen reacted with the hematite samples, allowing the sample to reach 100% reduction degree within 2000s at 1023K-1273K. If 10% water vapor was mixed into hydrogen as gas reactant for reduction reaction, the maximum reduction degree would be

reduced from 100% to 96.6% at 1023K, but had no effect at the other experimental temperatures. Continuing to increase the water vapor content to 20%, the maximum reduction degree would continue to decrease to 83.3% at 1023K and from 100% to 95.6% at 1073K. However, when the water vapor content of the hydrogen-water vapor gas mixture increased to 50%, the maximum reduction degree was only 25.1% at 1023K, but as the experimental temperature increased, the maximum reduction

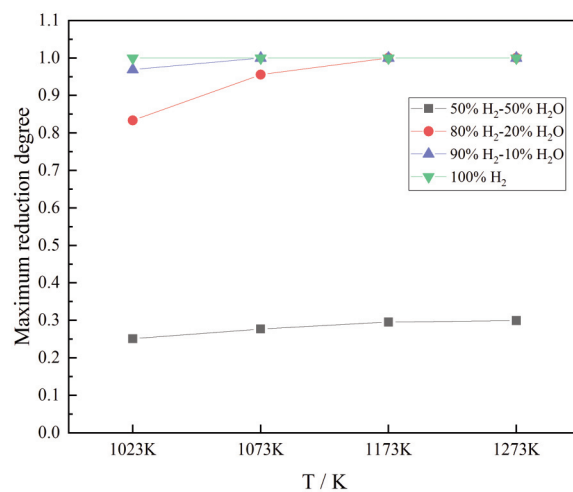


Figure 6. Maximum reduction degree under different reaction conditions



degree of the sample also increased. The maximum reduction degree at 1173K was 29.5% and remained basically unchanged if the temperature was continued to increase.

### 3.3. Effect of water on the reaction rate

As mentioned above, the entire reduction reaction process was artificially divided into three stages, each of which corresponds to a main reaction. In the stage 1 ( $0 \leq X \leq 0.11$ ) of reduction reaction, hematite was reduced to magnetite. From the thermodynamic conditions of the reaction, it can be seen that this reaction can easily occur with low hydrogen partial pressure under the premise of the experimental temperature. Since the minimum hydrogen partial pressure in the experimental conditions was also much higher than the theoretical critical hydrogen partial pressure, water vapor had relatively small effect on the reaction rate at this stage. The average reaction rate of the stage 1 of the reduction reaction is shown in Figure 7. The average reaction rate dropped by 53.6% when the water vapor content of gas reactant rose from 0% to 50% at 1023K, but the average reaction rate only dropped by 25.5% when the water vapor content rose to only 20%. When the reaction temperature increased to 1273K, the average reaction rate dropped by only 17.3% and the water vapor content was also 20% at this point, but this time the average reaction rate decreased to the highest degree at 0.00181.

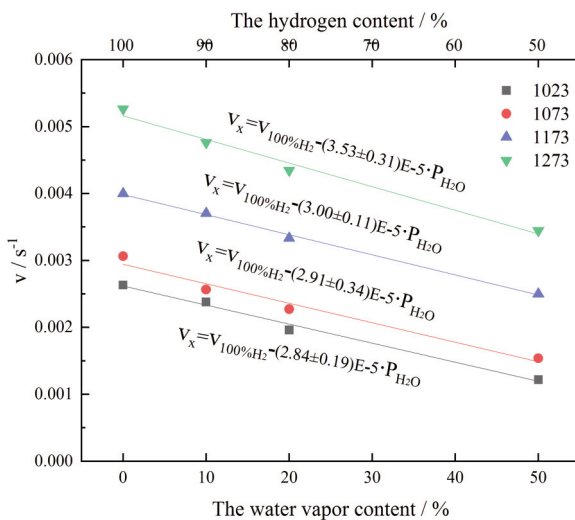


Figure 7. The relationship between water vapor content and average reduction rate in stage 1

As the reaction progressed to the stage 2 ( $0.11 \leq X \leq 0.33$  when water vapor content  $\leq 20\%$ ,  $0.11 \leq X \leq 0.2$  when water vapor content = 50%), the main reaction in this stage was transformed into a reaction from magnetite to wustite. The main reaction

in this stage was thermodynamically relatively difficult to proceed compared to the reaction in the stage 1. Therefore, the water vapor content in hydrogen-water vapor gas mixture had a greater impact on the reaction rate, and the specific results are shown in Figure 8. When the reduction temperature was 1023K, the average reaction rate decreased with increasing water vapor content in gas reactant. However, with the increase of reaction temperature, the decrease rate of average reaction rate would be faster, as shown by the slope of the linear fit becoming smaller as the temperature increased. Besides, as the reaction temperature increased, the average reaction rate also increased. If the experimental temperature was increased to 1273K, the average reaction rate at 50% water vapor content would be higher than that of pure hydrogen at 1023K.

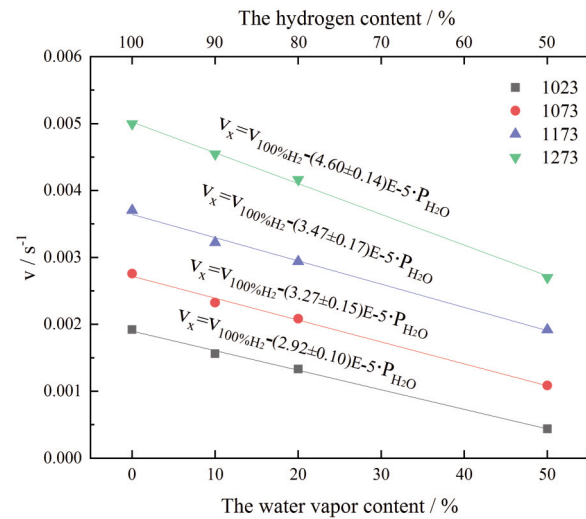


Figure 8. The relationship between water vapor and average reduction rate in stage 2

Figure 9 shows the effect of water vapor content on average reaction rate of stage 3 prophase ( $0.33 \leq X \leq 0.8$ ) of reduction reaction. For 50% water vapor content the reduction reaction could not react in stage 3, while for the pure hydrogen the reduction degree rapidly reached 0.9 without obvious deceleration. Under the same experimental temperature, the average reaction rate decreased approximately linearly with the increase of water vapor content. When the water vapor content increased from 0% to 20% at 1023K, the average reaction rate dropped the most, which was about 78.1%. However, if it was in stage 2 of the reduction reaction, the average rate dropped at most only by about 30.7% at 1023K. Those results show the content of water vapor in the gas reactant has a great influence on the final stage of reduction reaction consistent with previous studies [24-26]. Furthermore, the average reaction rate increased almost linearly with the



increase of the reaction temperature at the same water vapor content.

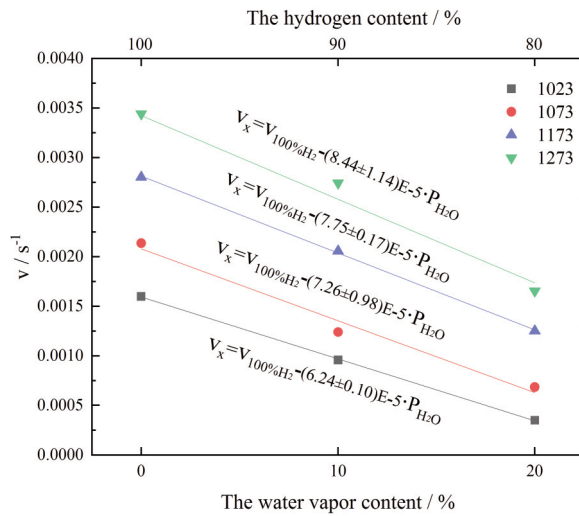


Figure 9. The relationship between water vapor and average reduction rate in stage 3

All in all, water vapor has different effects at different stages of reduction reaction, which is reflected in reaction thermodynamics and kinetics. On the basis of thermodynamics, since water vapor is the substance produced by the reduction reaction, the large amount of water vapor will cause Delta G of the reaction to increase, and the tendency of the forward reaction to decrease. In terms of kinetics, since the viscosity of water vapor at the same temperature is greater than that of hydrogen, this will cause the gas diffusion coefficient of the gas reactant to decrease, making gas mass transfer difficult [27-28].

### 3.4. Effect of water on the apparent activation energy

The isothermal reaction rate ( $dX/dt$ ) is also obtained by the differentiation of the degree of reaction to the reaction time, which is a function of rate constant of reaction ( $k$ ) and the reaction mechanism model function ( $f(X)$ ) that has a certain transformation relationship with time  $t$ .

$$\frac{dX}{dt} = k \cdot f(X) \quad (7)$$

$$F(X) = \int_0^X \frac{dX}{f(X)} \quad (8)$$

where  $F(X)$  is the integral reaction model. Separating variables and integrating Eq 7 and Eq 8 gives the integral forms of the isothermal rate law.

$$F(X) = k \cdot t \quad (9)$$

Table 2 [29-32] presents the suggested mathematical functions used for the reaction kinetic model, which covers most of possible mechanisms that control the reduction reaction. Therefore, these functions will be used for mathematical modeling of reaction kinetic data, where the best fitting functions will be chosen to ultimately decide the reaction controlling mechanism.

Table 2. Reaction kinetic model functions applied for the solid-state reaction

| Model                                               | Integral Form                            | Differential Form                                         |
|-----------------------------------------------------|------------------------------------------|-----------------------------------------------------------|
|                                                     | $F(X) = \int_0^X \frac{dX}{f(X)}$        | $f(X) = \frac{dX}{dt} / k$                                |
| One-dimensional diffusion (D1)                      | $X^2$                                    | $\frac{1}{2X}$                                            |
| Two-dimensional diffusion (D2)                      | $(1-X)\ln(1-X) + X$                      | $-\frac{1}{\ln(1-X)}$                                     |
| Three-dimensional diffusion (Jander)                | $\left[1 - (1-X)^{\frac{1}{3}}\right]^2$ | $\frac{3(1-X)^{\frac{2}{3}}}{2[1 - (1-X)^{\frac{1}{3}}]}$ |
| Three-dimensional diffusion (Ginstling-Brounshtein) | $1 - \frac{2X}{3} - (1-X)^{\frac{2}{3}}$ | $\frac{3}{2[(1-X)^{\frac{1}{3}} - 1]}$                    |
| Zero-order (F0/R1)                                  | $X$                                      | $1$                                                       |
| First-order (F1)                                    | $-\ln(1-X)$                              | $1-X$                                                     |
| Second-order (F2)                                   | $\frac{1}{1-X} - 1$                      | $(1-X)^2$                                                 |
| Contracting area (R2)                               | $1 - (1-X)^{\frac{1}{2}}$                | $2(1-X)^{\frac{1}{2}}$                                    |
| Contracting volume (R3)                             | $1 - (1-X)^{\frac{1}{3}}$                | $3(1-X)^{\frac{1}{3}}$                                    |
| Avrami-Erofeyev (A2)                                | $[-\ln(1-X)]^{\frac{1}{2}}$              | $2(1-X)[- \ln(1-X)]^{\frac{1}{2}}$                        |
| Avrami-Erofeyev (A3)                                | $[-\ln(1-X)]^{\frac{1}{3}}$              | $3(1-X)[- \ln(1-X)]^{\frac{2}{3}}$                        |
| Avrami-Erofeyev (A4)                                | $[-\ln(1-X)]^{\frac{1}{4}}$              | $4(1-X)[- \ln(1-X)]^{\frac{3}{4}}$                        |

According to the above mention, the of the reaction was also divided into three stages for analysis. Figure 10 exhibits the mathematical modeling of contracting volume (R3) of the experimental data during the stage 3 with 80% $H_2$ -20% $H_2O$  gas mixture at 1023K to 1273K. The model generate correlation coefficient were greater than 0.99, which the slope of the model was the .

The rest experiment data deduced by analogy, which were fitted using the model of Three-dimensional diffusion (Jander) and Contracting volume (R3) in Table 2. According to Strangway study [33], as shown in Table 3, the probable rate controlling step of reaction can be speculated by obtaining the apparent activation energy ( $E_a$ ). Therefore, in order to preliminarily determine the



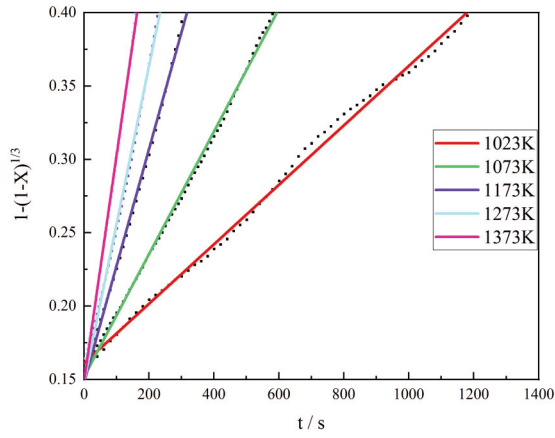


Figure 10. Application of the model of contracting volume (R3) at the stage of wustite reduction to metallic iron with 80% $H_2$ -20% $H_2O$  gas mixture

probable rate controlling mechanism of the three stages of the reduction reaction, the  $E_a$  of reduction should be obtained, which was calculated from following methods.

$$k = Ae^{\frac{-E_a}{RT}} \quad (10)$$

$$\ln k = \ln \left( Ae^{\frac{-E_a}{RT}} \right) = \ln A - \frac{E_a}{R} \cdot \frac{1}{T} \quad (11)$$

where  $k$ ,  $A$ ,  $R$ , are the rate constant of reaction, the preexponential (frequency) factor, the gas constant, respectively. The Arrhenius plots for the experiments are shown in the Figure 11.

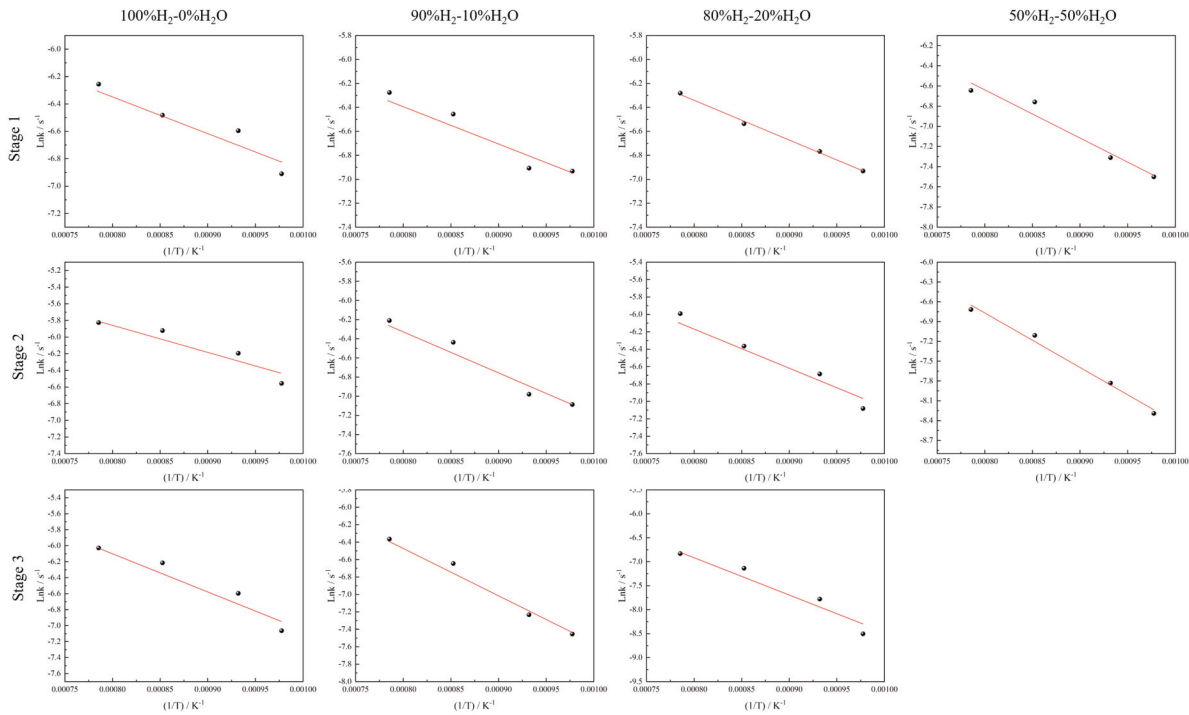


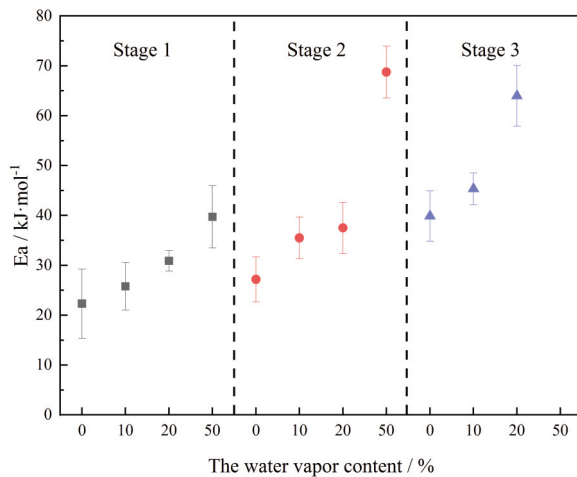
Figure 11. Arrhenius plots of the rate constant for the experiments

Table 3. Relationship between apparent activation energy and probable rate controlling step

| NO. | Apparent activation energy $E_a$ (kJ/mol) | Probable rate controlling step                           |
|-----|-------------------------------------------|----------------------------------------------------------|
| 1   | 8~16                                      | Gas diffusion                                            |
| 2   | 29~42                                     | Combined gas diffusion and interfacial chemical reaction |
| 3   | 60~67                                     | Interfacial chemical reaction                            |
| 4   | >90                                       | Solid-state diffusion                                    |

For the three stages of hematite reduction, the apparent activation energy of the reaction in each stage increased as the proportion of water vapor in the gas reactant increased. As shown in the Figure 12, in the stage 1 of hematite reduction, the apparent activation energy of the reaction slightly decreased as the water vapor content decreased. The activation energy obtained through the above analysis was basically in the range of 20kJ/mol to 40kJ/mol when the reaction was in the stage 1, which indicated that the probable rate controlling steps of reaction were gas diffusion or combined gas diffusion and interfacial chemical reaction. It was mainly reason that the  $\Delta G$  for the reduction of hematite to magnetite at this experimental condition was relatively small, but the mass transfer capacity of the

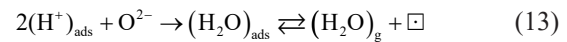
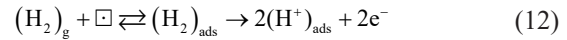




**Figure 12.** The apparent activation energy of three reaction stage

gas phase was relatively weak. In the stage 2 of reduction reaction, the apparent activation energy of the reaction was greater than in the stage 1. In the stage 3 of hematite reduction, the driving force of the reduction reaction continued to become smaller, and the kinetic condition of this early stage of reaction became better because the oxygen element in the sample was taken away by hydrogen in the stage 1 and 2 of reaction. Therefore, the apparent activation energy of the third stage of the reduction reaction would be significantly higher than the first two stages. When the proportion of water vapor in the gas reached 20%, the apparent activation energy of the reaction was about 64kJ/mol and the possible rate controlling step in the stage 3 of hematite reduction was interfacial chemical reaction. Moreover, when the

proportion of water vapor in the gas continued to increase to 50%, the hematite reduction can only proceed to the stage 2. At this stage can also be considered as the probable rate controlling step was interfacial chemical reaction. Moreover, during the reaction, water vapor would be adsorbed on the surface of the reactant, occupying active reaction sites [24, 34]. Once the active site on the sample was occupied, hydrogen cannot react at the active site, and sample “poisoning” occurs.



where  $\square$  and  $\blacksquare$  are the active reaction site and poisoning site. Besides, the mechanism of adsorption depends on temperature and a lower temperature is better for adsorption. With increasing temperature, the effect of water vapor adsorption decreases [20]. This is one of the reasons why the value of the apparent activation energy of the reaction is relatively large when the content of water vapor in the gas reactant is high.

The microstructure of reduction products with different gas reactant conditions at 1273K are shown in Figure 13. It seems that the high temperature did not cause serious sintering of the reduction products, and the reduction product still had some holes and cracks, where the channel for hydrogen diffusion was not seriously blocked, and the situation of relying only on solid-state mass transfer had not yet appeared.

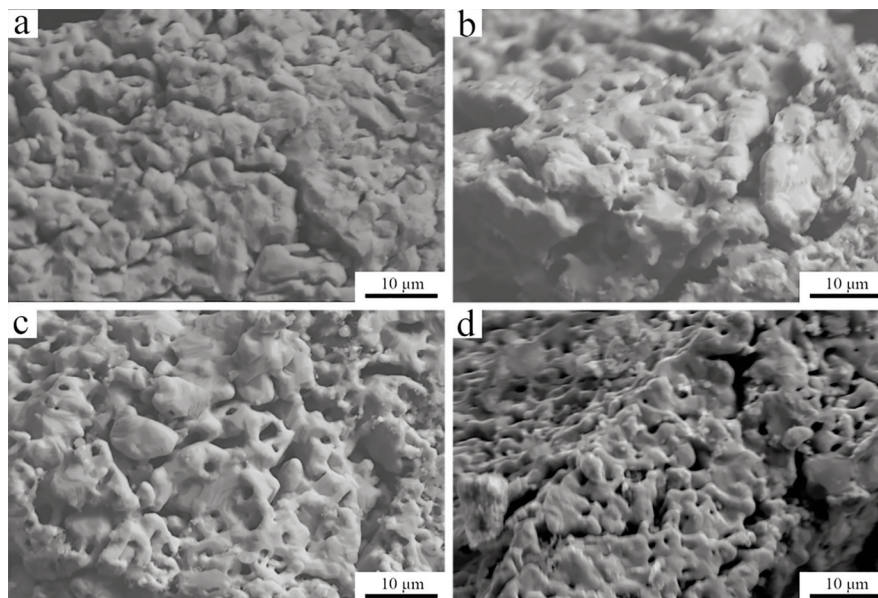


**Figure 13.** The microstructure of reduction products at 1273K with: (a) 50% $H_2$ -50% $H_2O$  (b) 80% $H_2$ -20% $H_2O$  (c) 90% $H_2$ -10% $H_2O$  (d) 100% $H_2$

The reduction product presented a relatively initial shape at 50% water vapor content in gas reactant, which it could only react to the stage 2. However, as the content of water vapor in gas reactant decreased, the reduction reaction reacted into the stage 3, and the morphology of the product also underwent further changes, which was formation of network structure with increased porosity and fully developed iron phase bonded with each other.

The raw materials of a reaction and its physical state and purity determine the value of the apparent activation energy of the reaction. In addition, for the same solid, different experimental conditions lead to different values of apparent activation energy. All these parameters have an influence on the rate-limiting step, and therefore, different rate-limiting steps lead to different apparent activation energies. By summarizing the results of previous studies, as given in Table 4 [33, 35-42], it can be found that the apparent activation energy obtained when the reaction experimental conditions are similar to the reaction conditions in this study are also relatively consistent.

**Table 4.** Apparent activation energy of iron oxides reduced to iron with hydrogen

| NO. | Material  | Temperature range (K) | Apparent activation energy (kJ/mol) | Remarks                                                      |
|-----|-----------|-----------------------|-------------------------------------|--------------------------------------------------------------|
| 1   | Hematite  | 973-1373              | 53.5                                | Dense briquettes                                             |
| 2   | Hematite  | 973-1373              | 21.5                                | Porous briquettes                                            |
| 3   | Wustite   | 1173-1373             | 53.8                                | 450 $\mu$ m                                                  |
| 4   | Hematite  | 773-1373              | 29.7                                | Green compacts                                               |
| 5   | Hematite  | 773-1374              | 41.0                                | Porous compacts                                              |
| 6   | Hematite  | 1173-1473             | 69.5                                | Cylindrical                                                  |
| 7   | Hematite  | 733-773               | 56.8                                | Pure Fe <sub>2</sub> O <sub>3</sub>                          |
| 8   | Hematite  | 738,758 and 778       | 52.7                                | 4% water vapor                                               |
| 9   | Hematite  | 738,758 and 779       | 55.2                                | 7.5% water vapor                                             |
| 10  | Hematite  | 573-773               | 30.1                                | pellets                                                      |
| 11  | Hematite  | 598-773               | 47.2                                | powder                                                       |
| 12  | Magnetite | 973-1273              | 42-55                               | 75-180 $\mu$ m                                               |
| 13  | Hematite  | 593-693               | 57.1                                | Pure Fe <sub>2</sub> O <sub>3</sub> (without heat treatment) |

#### 4. Conclusion

The reaction of the hematite sample with hydrogen and hydrogen-water vapor gas mixture was

studied with an accurate TGA at 1023K-1273K. The reduction results obtained by a series of comprehensive analyses and compared with previous researches can lead to the following conclusions:

1. The whole reduction process of hematite is divided into three stages. The content of water vapor in the gas reactant has the least influence on the first stage. The average reaction rate decreases only by 25.5% when the water vapor content decreases at 1023K from 0% to 20%, and with the increase of the reaction temperature, the degree of the decrease of the average reaction rate decreases further. As the reduction reaction of hematite progresses, the influence of water vapor in the reaction gas increases. In stage 3, when the water vapor content increases from 0% to 20% at 1023K, the average reaction rate decreases the most, by 78.1%. In addition, the influence of water vapor on the reduction reaction increases with increasing reaction temperature at all stages of the reduction reaction.

2. Under unfavorable reducing conditions, i.e., when that the reduction temperature is lower than 1173K and the water vapor content in the reducing atmosphere is higher than 20%, it is difficult to achieve a high degree of metallization within 2000s. Under the experimental conditions of this study, the reduction products of hematite can be taken from the SEM image that the sintering situation is not very serious, and a large number of cracks and holes can be seen. Combining the apparent activation energy of the reaction with the SEM image, it can be assumed that there is no rate controlling step dominated by solid-state diffusion.

3. By fitting the experimental results to the model and mutually confirming the apparent activation energy obtained from the experiment, it can be assumed that the probable rate controlling steps of the reaction at low water vapor content are gas diffusion or combined gas diffusion and interfacial chemical reaction. However, at high water vapor content the probable rate controlling steps of reaction are chemical reactions at the interface. Moreover, under the same experimental conditions, the apparent activation energy of the reaction increases as the reaction enters the next stage.

4. Water vapor will adversely affect the reduction reaction in both kinetics and thermodynamics. In thermodynamics, water vapor is a product, and affects the progress of the reaction. In terms of kinetics, water vapor impairs the diffusion of hydrogen and adsorbs on the active site to making it toxic. However, increasing the reaction temperature reduces the disadvantages caused by water vapor.

#### Acknowledgements

The authors were very grateful for the financial



support provided by State Key Laboratory of Advanced Metallurgy (University of Science and Technology Beijing, USTB).

### Author Contributions

*Conceptualization:* Kuochih Chou; *Methodology:* Xiaojun Hu; *Experimenting and Writing:* Xudong Mao and Yuewen Fan

### Data availability

The datasets used or analyzed during the current study are available from the corresponding author on reasonable request.

### Conflict of Interest

The authors declare that they have no conflict of interest.

### Reference

- [1] K. Onarheim, A. Mathisen, A. Arasto, Barriers and opportunities for application of CCS in Nordic industry—A sectorial approach, *International Journal of Greenhouse Gas Control*, 36 (2015) 93-105. <https://doi.org/10.1016/j.ijggc.2015.02.009>
- [2] Y. Rajshekar, J. Pal, T. Venugopalan, Development of hematite ore pellet utilizing mill scale and iron ore slime combination as additive, *Journal of Mining and Metallurgy, Section B: Metallurgy*, 52 (2) (2018) 197-208. <https://doi.org/10.2298/JMMB180116008R>
- [3] K.D. Burchart, Life cycle assessment of steel production in Poland: a case study, *Journal of Cleaner Production*, 54 (2013) 235-243. <https://doi.org/10.1016/j.jclepro.2013.04.031>
- [4] J. Dang, X.J. Hu, G.H. Zhang, X.M. Hou, X.B. Yang, K.C. Chou, Kinetics of reduction of Titano-magnetite powder by H<sub>2</sub>, *High Temperature Materials and Processes*, 32 (3) (2013) 229-236. <https://doi.org/10.1515/htmp-2012-0128>
- [5] J. Dang, G.H. Zhang, X.J. Hu, K.C. Chou, Non-isothermal reduction kinetics of Titano-magnetite by hydrogen, *International Journal of Minerals, Metallurgy and Materials*, 20 (2013) 1134-1140. <https://doi.org/10.1007/s12613-013-0846-9>
- [6] R.K. Dishwar, O.P. Sinha, Effect of partially reduced highly fluxed DRI pellets on impurities removal during steelmaking using a laboratory scale EAF, *Journal of Mining and Metallurgy, Section B: Metallurgy*, 58 (1) (2022) 63-73. <https://doi.org/10.2298/JMMB210319050D>
- [7] Z.Y. Chen, J. Dang, X.J. Hu, H.Y. Yan, Reduction kinetics of hematite powder in hydrogen atmosphere at moderate temperatures, *Metals*, 8 (2018) 751-760. <https://doi.org/10.3390/met8100751>
- [8] D.B. Guo, L.D. Zhu, S. Guo, B.H. Cui, S.P. Luo, Direct reduction of oxidized iron ore pellets using biomass syngas as the reducer, *Fuel Processing Technology*, 148 (2016) 276-281. <https://doi.org/10.1016/j.fuproc.2016.03.009>
- [9] W.H. Kim, S. Lee, S.M. Kim, The retardation kinetics of magnetite reduction using H<sub>2</sub> and H<sub>2</sub>-H<sub>2</sub>O mixtures, *International Journal of Hydrogen Energy*, 38 (10) (2013) 4194-4200. <https://doi.org/10.1016/j.ijhydene.2013.01.147>
- [10] F. Adam, F. Jeannot, B. Dupre, The remarkable effect of water vapour on the cracking of hematite during its reduction into magnetite, *Reactivity of Solids*, 5 (2) (1988) 115-127. [https://doi.org/10.1016/0168-7336\(88\)80081-0](https://doi.org/10.1016/0168-7336(88)80081-0)
- [11] M. Moukassi, M. Gougeon, P. Steinmetz, Hydrogen reduction of wustite single crystals doped with Mg, Mn, Ca, Al, and Si, *Metallurgical and Materials Transactions B*, 15 (1984) 383-391. <https://doi.org/10.1007/BF02667342>
- [12] P. Garg, X.J. Hu, Y. Li, K.J. Li, S. Nag, J.L. Zhang, Kinetics of iron oxide reduction in H<sub>2</sub>/H<sub>2</sub>O gas mixture: global and stepwise reduction, *Metallurgical and Materials Transactions B*, 53 (2022) 1759-1774. <https://doi.org/10.1007/s11663-022-02485-7>
- [13] R. Steffen, K.H. Tacke, W. Pluschkell, Grundlagenuntersuchungen zur umweltfreundlichen Reduktion von Eisenerz mit Wasserstoff oder wasserstoffreichen Gemischen, Europäische Kommission, Luxemburg, 1998, p85.
- [14] W.K. Jozwiak, E. Kaczmarek, T.P. Maniecki, Reduction behavior of iron oxides in hydrogen and carbon monoxide atmospheres, *Applied Catalysis A: General*, 326 (1) (2007) 17-27. <https://doi.org/10.1016/j.apcata.2007.03.021>
- [15] A.J. Kock, H.M. Fortuin, J.W. Geus, The reduction behavior of supported iron catalysts in hydrogen or carbon monoxide atmospheres, *Journal of Catalysis*, 96 (1) (1985) 261-275. [https://doi.org/10.1016/0021-9517\(85\)90379-3](https://doi.org/10.1016/0021-9517(85)90379-3)
- [16] H.Y. Lin, Y.W. Chen, C. Li, The mechanism of reduction of iron oxide by hydrogen, *Thermochimica Acta*, 400 (1) (2003) 61-67. [https://doi.org/10.1016/S0040-6031\(02\)00478-1](https://doi.org/10.1016/S0040-6031(02)00478-1)
- [17] P. Pourghahramani, E. Forssberg, Reduction kinetics of mechanically activated hematite concentrate with hydrogen gas using nonisothermal methods, *Thermochimica Acta*, 454 (2) (2007) 69-77. <https://doi.org/10.1016/j.tca.2006.12.023>
- [18] L.V. Bogdandy, H.J. Engell, Die Reduktion der Eisenerze, Heidelberg, Berlin, 1967, p31.
- [19] B. Weiss, J. Sturn, F. Winter, J.L. Schenk, Empirical reduction diagrams for reduction of iron ores with H<sub>2</sub> and CO gas mixtures considering non-stoichiometries of oxide phases, *Ironmaking & Steelmaking*, 36 (3) (2009) 212-216. <https://doi.org/10.1179/174328108X380645>
- [20] D. Spreitzer, J. Schenk, Reduction of iron oxides with hydrogen—a review, *Steel Research International*, 90 (10) (2019) 1900108. <https://doi.org/10.1002/srin.201900108>
- [21] A.A. El-Geassy, V. Rajakumar, Gaseous reduction of wustite with H<sub>2</sub>, CO and H<sub>2</sub>-CO mixtures, *Transactions of the Iron & Steel Institute of Japan*, 25 (6) (1985) 449-458. <https://doi.org/10.2355/isijinternational1966.25.449>
- [22] J. Zhang, O. Ostrovski, Iron ore reduction/cementation: experimental results and kinetic modelling, *Ironmaking & Steelmaking*, 29 (1) (2002) 15-21. <https://doi.org/10.1179/030192302225001929>
- [23] E. Lorente, J. Herguido J.A. Peña, Steam-iron process:



- Influence of steam on the kinetics of iron oxide reduction, *International Journal of Hydrogen Energy*, 36 (21) (2011) 13425-13434. <https://doi.org/10.1016/j.ijhydene.2011.07.111>
- [24] O.J. Wimmers, P. Arnoldy, J.A. Moulijn. Determination of the reduction mechanism by temperature-programmed reduction: application to small iron oxide ( $\text{Fe}_2\text{O}_3$ ) particles, *Journal of Physical Chemistry*, 90 (7) (1986) 1331-1337. <https://doi.org/10.1021/j100398a025>
- [25] A. Baranski, J.M. Lagan, A. Pattek, A. Reizer, The effect of water on the reduction of an iron catalyst for ammonia synthesis, *Applied Catalysis*, 3 (3) (1982) 201-206. [https://doi.org/10.1016/0166-9834\(82\)85001-X](https://doi.org/10.1016/0166-9834(82)85001-X)
- [26] A. Baranski, A. Kotarba, J.M. Lagan, Kinetics of wet atmosphere reduction of a fused iron catalyst for ammonia synthesis, *Applied Catalysis*, 71 (2) (1991) L1-L4. [https://doi.org/10.1016/0166-9834\(91\)85078-A](https://doi.org/10.1016/0166-9834(91)85078-A)
- [27] I.J. Moon, C.H. Rhee, M. Dongjoon. Reduction of hematite compacts by  $\text{H}_2$ -CO gas mixtures, *Steel Research*, 69 (8) (1998) 302-306. <https://doi.org/10.1002/srin.199805555>
- [28] L.Y. Xing, Z.S. Zou, Y.X. Qu, Gas-solid reduction behavior of in-flight fine hematite ore particles by hydrogen, *Steel Research International*, 90 (1) (2019) 1800311. <https://doi.org/10.1002/srin.201800311>
- [29] A. Khawam, D.R. Flanagan, Solid-state kinetic models: basics and mathematical fundamentals, *The Journal of Physical Chemistry B*, 110 (35) (2006) 17315-17328. <https://doi.org/10.1021/jp062746a>
- [30] A. Ortega, The kinetics of solid-state reactions toward consensus—Part I: Uncertainties, failures, and successes of conventional methods, *International Journal of Chemical Kinetics*, 33 (2001) 343-353. <https://doi.org/10.1002/kin.1028>
- [31] B. Janković, B. Adnadević, J. Jovanović, Application of model-fitting and model-free kinetics to the study of non-isothermal dehydration of equilibrium swollen poly (acrylic acid) hydrogel: thermogravimetric analysis, *Thermochimica Acta*, 425 (2) (2007) 106-115. <https://doi.org/10.1016/j.tca.2006.07.022>
- [32] G. Munteanu, P. Budrugaec, Kinetics of temperature programmed reduction of  $\text{Fe}_3\text{O}_4$  promoted with copper: application of iso-conversional methods, *Journal of Materials Science*, 38 (2003) 1995-2000. <https://doi.org/10.1023/A:1023589405546>
- [33] M.I. Nasr, A.A. Omar, M.H. Khedr, Effect of nickel oxide doping on the kinetics and mechanism of iron oxide reduction, *ISIJ International*, 35 (9) (1995) 1043-1049. <https://doi.org/10.2355/isijinternational.35.1043>
- [34] M. Moukassi, P. Steinmetz, B. Dupre, C. Gleitzer, A study of the mechanism of reduction with hydrogen of pure wustite single crystals, *Metallurgical and Materials Transactions B*, 14 (1983) 125-132. <https://doi.org/10.1007/BF02670879>
- [35] A.A. El-Geassy, K.A. Shehata, S.Y. Ezz, Mechanism of iron oxide reduction with hydrogen/carbon monoxide mixtures, *Transactions of the Iron and Steel Institute of Japan*, 17 (11) (1977) 629-635. <https://doi.org/10.2355/isijinternational1966.17.629>
- [36] A.A. El-Geassy, V. Rajakumar, Influence of particle size on the gaseous reduction of wustite at 900-1100°C, *Transactions of the Iron and Steel Institute of Japan*, 25 (12) (1985) 1202-1211. <https://doi.org/10.2355/isijinternational1966.25.1202>
- [37] A.A. El-Geassy, M.I. Nasr, Influence of original structure on the kinetics and mechanisms of carbon monoxide reduction of hematite compacts, *ISIJ International*, 30 (6) (1990) 417-425. <https://doi.org/10.2355/isijinternational.30.417>
- [38] A. Pineau, N. Kanari, I. Gaballah, Kinetics of reduction of iron oxides by  $\text{H}_2$ : Part I: Low temperature reduction of hematite, *Thermochimica Acta*, 447 (1) (2006) 89-100. <https://doi.org/10.1016/j.tca.2005.10.004>
- [39] M.H.A. Elhamid, M.M. Khader, A.E. Mahgoub, Autocatalytic reduction of hematite with hydrogen under conditions of surface control: a vacancy-based mechanism, *Journal of Solid State Chemistry*, 123 (2) (1996) 249-254. <https://doi.org/10.1006/jssc.1996.0175>
- [40] G.Y. Lee, J.P. Choi, J.I. Song, The kinetics of isothermal hydrogen reduction of nanocrystalline  $\text{Fe}_2\text{O}_3$  powder, *Materials Transactions*, 55 (10) (2014) 1611-1617. <https://doi.org/10.2320/matertrans.M2014182>
- [41] S.K. Kuila, R. Chatterjee, D.Ghosh, Kinetics of hydrogen reduction of magnetite ore fines, *International Journal of Hydrogen Energy*, 41 (22) (2016) 9256-9266. <https://doi.org/10.1016/j.ijhydene.2016.04.075>
- [42] M.V.C. Sastri, R.P. Viswanath, B. Viswanathan, Studies on the reduction of iron oxide with hydrogen, *International Journal of Hydrogen Energy*, 7 (12) (1982) 951-955. [https://doi.org/10.1016/0360-3199\(82\)90163-X](https://doi.org/10.1016/0360-3199(82)90163-X)



## UTICAJ VODENE PARE NA KINETIKU REDUKCIJE HEMATITNOG PRAHA UZ POMOĆ VODONIKA-VODENE PARE U RAZLIČITIM FAZAMA

X.-D. Mao, X.-J. Hu\*, Y.-W. Fan, K.-C. Chou

Univerzitet za nauku i tehnologiju u Pekingu, Glavna državna laboratorija za naprednu metalurgiju, Peking,  
NR Kina

### Apstrakt

Prah uzorka hematita je izotermno redukovan mešavinom gasa vodonik/vodena para na 1023K-1273K. Rezultati ukazuju da se ukupan proces redukcije hematita može podeliti u tri faze ( $Fe_2O_3$ - $Fe_3O_4$ - $FeO$ - $Fe$ ), od kojih svaku treba istražiti. Na 1023K, prosečna brzina reakcije je smanjena za 53,6% u fazi 1 kada se sadržaj vodene pare u reakcionom gasu povećao sa 0% na 50%, i za oko 77,2% u fazi 2. Međutim, u fazi 3, kada se sadržaj vodene pare povećao sa 0% samo na 20%, sadržaj se smanjio za oko 78,1%. Rezultati takođe pokazuju da se uticaj vodene pare na reakciju redukcije povećava sa povećanjem temperature reakcije u svim fazama reakcije redukcije. Mikrostruktura proizvoda redukcije pokazala je da su još uvek postojale neke šupljine, što nije ozbiljno blokiralo put za difuziju vodonika. Razmatrani su različiti modeli kako bi se dodatno razjasnio uticaj vodene pare u fazi redukcije. Opseg prividne energije aktivacije različitih faza dobijenih prilagođavanjem modela bio je oko 20-70 kJ/mol, što je takođe potvrdilo odsustvo fenomena difuzije u čvrstom stanju.

**Ključne reči:** Redukcija; Voda; Vodonik; Kinetički mehanizam

